

## Mathematical model of electric drive for rolling mill

**Abstract.** In the paper the analysis of electromechanical processes in drive system for rolling mill with rigid torque transmission is presented. The abovementioned drive system, that bases on lumped parameters, consists of two high-power induction motors driving the rolls of rolling mill. The method based on the modification of Hamilton's principle was used in order to formulate the state differential equations. The numerical simulations of the rolling-mill operation are made for three examples. The results are presented as graphs.

**Streszczenie.** W pracy poddano analizie procesy elektromechaniczne w układzie napędowym walcarki o sztywnej transmisji ruchu. Badany układ składa się z dwóch silników indukcyjnych dużej mocy, które napędzają cylindry walcarki. System rozpatruje się jako układ o parametrach skupionych. Dla formowania różniczkowych równań stanu wykorzystano metodę, która bazuje na modyfikacji zasady Hamiltona. Przeprowadzono symulacje numeryczne pracy układu walcarki dla trzech przypadków obliczeniowych. Wyniki przedstawiono w postaci graficznej (**Model matematyczny napędu elektrycznego walcarki**).

**Słowa kluczowe:** zasada Hamiltona, Euler-Lagrange'a system, układ dwumaszynowy, elektromechaniczne przetwarzanie energii, walcownia  
**Keywords:** Hamilton's rule, Euler-Lagrange's system, two-machine system, electromechanical energy conversion, steel mill

### Introduction

The drive system for rolling mill is a very complicated electromechanical system. The huge rotating masses and long shafts with large moments of inertia are the main feature thereof. Analysis and tests of the abovementioned systems are complicated and sometimes dangerous for service personnel and researchers [3]. Various methods of mathematical modelling, that take advantage of the fundamental laws of applied physics, are used in order to avoid this problem.

The paper proposes a simplified mathematical model of electromechanical system with absolutely rigid torque transmission. On the basis of this model the electromechanical processes may be analyzed, especially the processes occurring in electromagnetic part. The main advantage of this model is the property that the analysis of function dependences of the system may be carried out in a simple manner, without integration of complicated equations describing the rolling mill mechanical part [1,2,3].

The extended functional of operation by Hamilton, obtained as a result of formulating the elements of modified Lagrangian, was used in order to obtain the mathematical model of electromechanical system. Then, the functional variation was determined and compared to zero. The extreme function equations of the abovementioned functional, obtained in this way, are the mathematical model of the power system.

### Mathematical model

The electromechanical system (Fig. 1), consisting of two induction motors that rotate the rollers by absolutely rigid shafts, is analyzed.

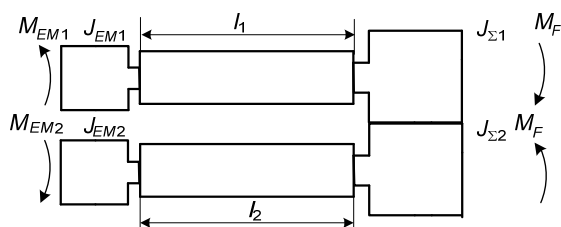


Fig. 1 Kinematic model of the rolling mill

The modified Lagrangian [1,2] is described by the equation:

$$(1) \quad L^* = \tilde{T}^* - P^* + \Phi^* - D^*,$$

where  $L^*$  is the modified Lagrange's function,  $\tilde{T}^*$  is kinetic co-energy,  $P^*$  is potential energy,  $\Phi^*$  is dissipation energy,  $D^*$  is external forces energy [1,2]. The following generalized coordinates are assumed in the paper: electric charges in stator and rotor windings of both motors  $q_{1-12} = Q_{1-12}$ :  $Q_{jSA}, Q_{jSB}, Q_{jSC}, Q_{jRA}, Q_{jRB}, Q_{jRC}$ , where  $j=1,2$ , angles of rotation of both rotors and rotating part of load mechanism  $q_{13} = \gamma_1, q_{14} = \gamma_2$ . The currents in stator and rotor windings  $\dot{q}_{1-12}(t) = i_{1-12}(t)$  as well as the angular velocities of rotors and driven mechanism are assumed as generalized velocities  $\dot{q}_{13} = \omega_1, \dot{q}_{14} = \omega_2$ , respectively.

The elements of modified Lagrangian (1) are described as follows (Fig. 1) [1, 2]:

$$(2) \quad \tilde{T}^* = \sum_{n=1}^2 \sum_{j=1}^3 \left[ \int_0^{i_{nSj}} \Psi_{nSj} di_{nSj} + \int_0^{i_{nRj}} \Psi_{nRj} di_{nRj} \right] + \frac{(J_{EM1} + J_{\Sigma 1})\omega_1^2}{2} + \frac{(J_{EM2} + J_{\Sigma 2})\omega_2^2}{2}, \quad j = A, B, C,$$

$$(3) \quad P^* = 0, \quad \Phi^* = \sum_{n=1}^2 \sum_{j=1}^3 \int_0^t \frac{1}{2} (r_{nSj} i_{nSj}^2 + r_{nRj} i_{nRj}^2) d\tau,$$

$$(4) \quad D^* = \sum_{n=1}^2 \sum_{j=1}^3 \int_0^t u_{nSj} i_{nSj} d\tau + \int_0^t \int_0^{\omega_1} M_{F1}(\omega_1, \omega_2) d\omega_1 d\tau - \int_0^t \int_0^{\omega_2} M_{F2}(\omega_1, \omega_2) d\omega_2 d\tau,$$

where  $S, R$  are stator and rotor indexes,  $\Psi$  is flux linkage  $r_S, r_R$  are resistances of stator and rotor windings,  $u_S$  is stator phase voltage,  $M_F$  is active load torque, incl. coefficient of friction.

The modified Lagrangian was formulated on the basis of the equations (2) - (4) and then the functional of operation by Hamilton was determined [2]. The Euler-Lagrange's equations were obtained as a consequence of derivation of functional variations [1], [2]:

$$(5) \quad \frac{d\Psi_{nS}}{dt} + r_{nS} i_{nj} - u_{nS} = 0,$$

$$(6) \quad \frac{d\Psi_{nR}}{dt} + r_{nR} i_{nR} = 0, \quad n = 1, 2,$$

$$(7) \quad \frac{d\omega_1}{dt} = \frac{1}{J_{EM1} + J_{\Sigma 1}} (M_{EM1} - M_{F1}),$$

$$(8) \quad \frac{d\omega_2}{dt} = \frac{1}{J_{EM2} + J_{\Sigma 2}} (M_{EM2} - M_{F2}),$$

Taking into account the equations of non-varying constraints, the mathematical model of two induction motors was obtained [1, 2]

$$(9) \quad \frac{d\mathbf{i}_{nS}}{dt} = \mathbf{A}_{nS}(\mathbf{u}_{nS} - \mathbf{r}_{nS}\mathbf{i}_{nS}) + \mathbf{A}_{nSR}(-\mathbf{\Omega}_{nR}\mathbf{\Psi}_{nR}^{\Pi} - \mathbf{r}_{nR}\mathbf{i}_{nR}^{\Pi}),$$

$$(10) \quad \frac{d\mathbf{i}_{nR}^{\Pi}}{dt} = \mathbf{A}_{nRS}(\mathbf{u}_{nS} - \mathbf{r}_{nS}\mathbf{i}_{nS}) + \mathbf{A}_{nR}(-\mathbf{\Omega}_{nR}\mathbf{\Psi}_{nR}^{\Pi} - \mathbf{r}_{nR}\mathbf{i}_{nR}^{\Pi}), \quad n=1, 2$$

$$(11) \quad \begin{bmatrix} i_A & i_B \end{bmatrix}^T = \begin{bmatrix} i_{SA} & i_{SB} \end{bmatrix}^T + \mathbf{\Pi} \begin{bmatrix} i_{RA} & i_{RB} \end{bmatrix}^T = \begin{bmatrix} i_{SA} & i_{SB} \end{bmatrix}^T + \begin{bmatrix} i_{RA}^{\Pi} & i_{RB}^{\Pi} \end{bmatrix}^T, \quad \tau = \frac{1}{L_m} = \left( \frac{\Psi_m}{i_m} \right)^{-1}; \quad \rho = \left( \frac{\partial \Psi_m}{\partial i_m} \right)^{-1},$$

$$(12) \quad i_m = 2\sqrt{(i_A^2 + i_A i_B + i_B^2)/3}, \quad b = \frac{2}{3} \frac{R-B}{L_m},$$

$$(13) \quad \Psi_m = 2\sqrt{(\Psi_A^2 + \Psi_A \Psi_B + \Psi_B^2)/3}, \quad b_A = b(2i_A + i_B),$$

$$(14) \quad B = 1/(\alpha_{\sigma S} + \alpha_{\sigma R} + \tau), \quad 1/(\alpha_{\sigma S} + \alpha_{\sigma RL} + \rho),$$

$$(15) \quad b_B = b(2i_B + i_A), \quad \mathbf{a}_{\sigma S} = \mathbf{L}_{\sigma S}^{-1}, \quad \mathbf{a}_{\sigma RL} = \mathbf{L}_{\sigma RL}^{-1},$$

$$(16) \quad \mathbf{\Pi} = \frac{2}{\sqrt{3}} \begin{bmatrix} \sin(\varphi_1 + 120^\circ) & -\sin \varphi_1 \\ \sin \varphi_1 & -\sin(\varphi_1 - 120^\circ) \end{bmatrix}, \quad \det \mathbf{\Pi} \neq 0,$$

$$(17) \quad \mathbf{\Omega} = \mathbf{\Pi} \frac{d\mathbf{\Pi}^{-1}}{dt} \equiv \frac{d\mathbf{\Pi}^{-1}}{dt} \mathbf{\Pi} \equiv -\mathbf{\Pi}^{-1} \frac{d\mathbf{\Pi}}{dt} = \frac{\omega}{\sqrt{3}} \begin{bmatrix} 1 & 2 \\ -2 & -1 \end{bmatrix},$$

$$(18) \quad \mathbf{G}_S = \mathbf{a}_{\sigma S} \mathbf{G}, \quad \mathbf{G}_R = \mathbf{a}_{\sigma RL} \mathbf{G} \mathbf{\Pi}, \quad \mathbf{G} = \begin{bmatrix} B + b_A i_A & b_B i_A \\ b_A i_B & B + b_B i_B \end{bmatrix},$$

$$(19) \quad \mathbf{A}_S = \mathbf{a}_{\sigma S} (\mathbf{I} - \mathbf{a}_{\sigma S} \mathbf{G}), \quad \mathbf{A}_{SR} = -\mathbf{a}_{\sigma S} \mathbf{a}_{\sigma RL} \mathbf{G} \mathbf{\Pi},$$

$$(20) \quad \mathbf{A}_{RS} = -\mathbf{\Pi}^{-1} \mathbf{a}_{\sigma S} \mathbf{a}_{\sigma RL} \mathbf{G}, \quad \mathbf{A}_R = \mathbf{\Pi}^{-1} \mathbf{a}_{\sigma RL} (\mathbf{I} - \mathbf{a}_{\sigma RL} \mathbf{G}) \mathbf{\Pi},$$

where:  $\mathbf{A}$  is matrix of coefficients depending on motor inductances,  $\mathbf{\Pi}$  indicates the transformed oblique coordinates [2],  $L_{\sigma S}$  is stator leakage inductance,  $L_{\sigma R}$  is rotor leakage inductance.

The electromagnetic torques of induction motors are derived from the following equation:

$$(21) \quad M_{nEM} = \sqrt{3} p_{n0} (i_{nSB} i_{nRA}^{\Pi} - i_{nSA} i_{nRB}^{\Pi}) / \tau_n,$$

where  $p_0$  is number of pole pairs,  $\tau$  is static inverse inductance of motor.

The differential equations (7) – (10) should be integrated together taking into account the dependencies (11) – (21).

### Computer simulation results

The transient states of a high-power rolling mill were analyzed. The kinematic diagram of the rolling mill is shown in Fig. 1. The analyzed electromechanical system consists of: two induction motors with data  $U_N = 6000$  V,  $f_N = 50$  Hz,  $P_N = 6300$  kW,  $n_N = 139$  obr/min,  $p = 20$ ,  $R_1 = 0,0808 \Omega$ ,  $R_2' = 0,0906 \Omega$ ,  $R_{Fe} = 481,70 \Omega$ ,  $L_m = 0,0587$  H,  $L_{\delta 1} = 1,135$  mH,  $L_{\delta 2} = 1,135$  mH,  $J_S = 2200$  kgm<sup>2</sup>, as well as the mechanical system, including: motor clutch with dimensions:  $d_{sr} = 1200$  mm,  $l = 1400$  mm, main joint with dimensions:  $d = 800$  mm,  $l = 12000$  mm, articulated joints

with dimensions:  $d = 800$  mm,  $l = 3200$  mm, ends of shafts of working rollers with dimensions:  $d = 450$  mm,  $l = 1800$  mm, ends of shafts of backing rollers with dimensions:  $d = 450$  mm,  $l = 1800$  mm, working roller with dimensions:  $d = 600$  mm,  $l = 2500$  mm, backing roller with dimensions:  $d = 800$  mm,  $l = 2500$  mm,  $J_{\Sigma 1} = J_{\Sigma 2} = 18900$  kg·m<sup>2</sup>.

The simulations of transient processes in rolling mill-based electromechanical system were made. Three examples were considered. The load torque of the started rolling-mill was equal to 10% of the rated torque (idle run) at the reduced feeding voltage. After reaching the set speed of motor, the voltage was increased to the rated value. Then the mill was loaded by working torque. After time  $t$  the load decreased to 10% of rated torque. The abovementioned examples differ in value of working torque: for the first example (I) this torque is equal to 70% of rated torque, for the second one (II) – 100%, and for the third one (III) - 130%.

Numerical calculations were made with the use of the own programs written in Visual FORTRAN.

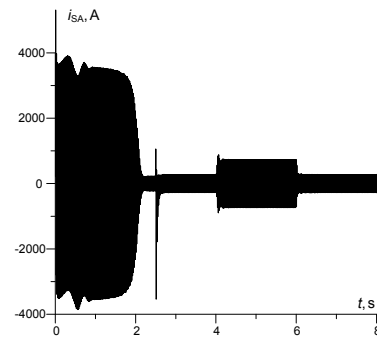


Fig. 2. Time-changes of stator A-phase current of the first motor for the first example

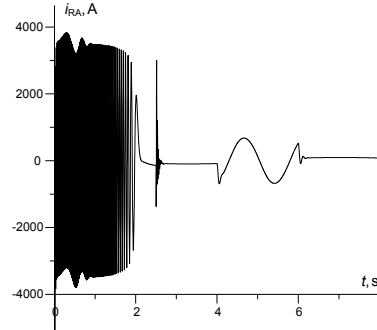


Fig. 3. Time-changes of rotor A-phase current in stator terms for the first example

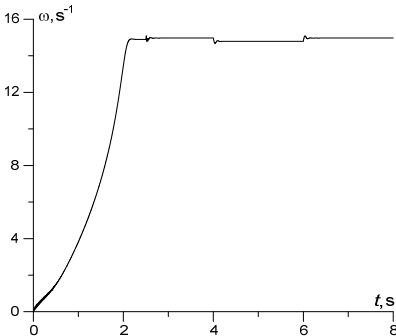


Fig. 4. Time-changes of rotor angular velocity of the first motor for the first example

Figs 2 to 5 show time-changes of: stator A-phase current, rotor A-phase current in stator terms, angular velocity of the first roll and electromagnetic torque of the

first induction motor, respectively, for the first example. For interval  $t_1 \in [0; 2,5]$  s starting the motor was simulated at the reduced voltage. For interval  $t_2 \in [2,5; 4]$  s the motor ran idle. For interval  $t_3 \in [4; 6]$  s the working torque was applied to the motor shaft. At the end, for interval  $t_4 \in [6; 8]$  s, the motor ran idle again.

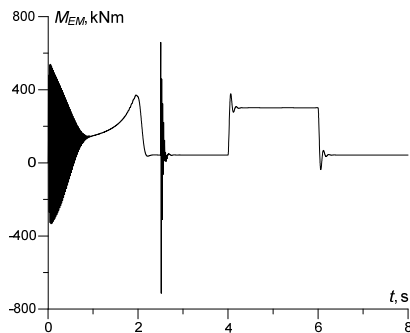


Fig. 5. Time-changes of electromagnetic torque of the first motor for the first example

Fig. 6 shows time-changes of electromagnetic torque of the first motor for the second example. For interval  $t_3 \in [4; 6]$  s, the working torque increases in comparison with Fig. 5, whereas, for the other intervals the torques are the same.

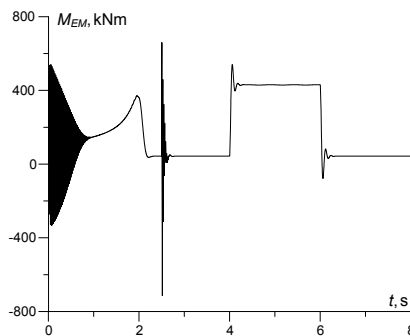


Fig. 6. Time-changes of electromagnetic torque of the first motor for the second example

Figures 7 to 9 show time-changes of: stator A-phase current, angular velocity of the first roll and electromagnetic torque of the first motor, respectively, for the third example. Comparing the abovementioned Figures with Figures 2, 4, 5, respectively, it can be noted that all the function dependencies increase if the motor is loaded. With regard to the second roller, all the function quantities are mirror images of the presented function quantities of the first roll.

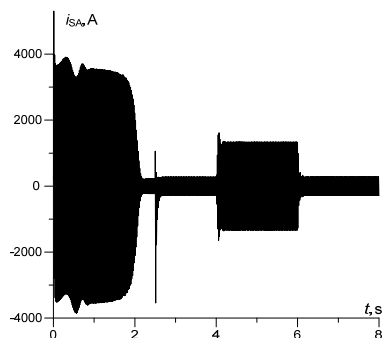


Fig. 7. Time-changes of stator A-phase current of the first motor for the third example

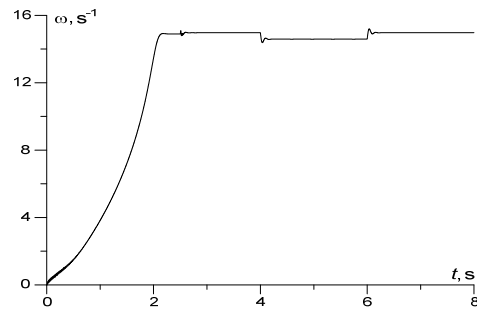


Fig. 8. Time-changes of rotor angular velocity of the first motor for the third example

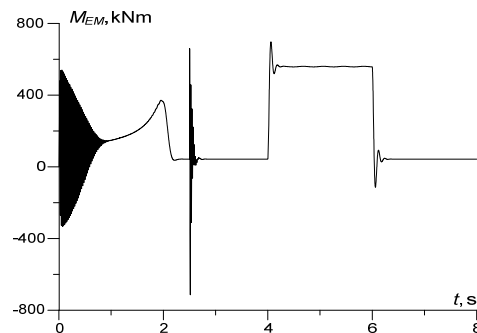


Fig. 9. Time-changes of electromagnetic torque of the first motor for the third example

## Conclusions

- On the basis of variational method, presented in the paper, the mathematical model of rolling mill-based electromechanical system with a rigid torque transmission was formulated. This method bases on the extended functional of operation by Hamilton.
- Using the formulated mathematical model and numerical methods, the simulation of rolling-mill operation were performed. The results are shown as time-changes that allow to analyze transient states in electromechanical system.
- The analysis of computer simulation results allows to avoid the faults of electromechanical systems at the stage of design efforts and during system operation.

## REFERENCES

- [1] Czaban A., Modelowanie matematyczne procesów oscylacyjnych systemów elektromechanicznych, wydanie drugie, zmienione i uzupełnione – Lwów: W-wo T. Soroki 2008.
- [2] Lis M., Modelowanie matematyczne procesów przejściowych w elektrycznych układach napędowych o złożonej transmisji ruchu, Seria monografie, Wydawnictwo Politechniki Częstochowskiej, Częstochowa 2013,
- [3] Rusek A., Stany dynamiczne układów napędowych z silnikami indukcyjnymi specjalnego wykonania, Seria Monografie 228, Wydawnictwo Politechniki Częstochowskiej, 2012.
- [4] Rusek A., Czaban A., Lis M., A Mathematical Model of a Synchronous Drive with Protrude Poles, An Analysis Using Variational Methods. SAEM'12. Digest Book of the 4th Symposium on Applied Electromagnetics. Ed. Miklos Kuczmann. June 3-6, 2012, Sopron, Hungary. s.79-80 ISBN 978-963-9819-85-6.
- [5] Ziemiński R.: Analiza drgań swobodnych pełnego układu dyskretno-ciągłego typu // Zesz. Nauk. A.G.H. – 1980. – Ne 775. – S. 177 – 188.
- [6] Puchala A.: Elektromechaniczne przetworniki energii, BOBRME Komel, Katowice 2002

**Autorzy:** prof. dr hab. inż. Andrzej Rusek, E-mail: [rusek@el.pcz.czest.pl](mailto:rusek@el.pcz.czest.pl); prof. nadzw. dr hab. inż. Andriy Czaban, E-mail: [atchaban@gmail.com](mailto:atchaban@gmail.com); dr. hab. inż. Marek Lis Politechnika Częstochowska, E-mail: [lism@el.pcz.czest.pl](mailto:lism@el.pcz.czest.pl); mgr inż. Marek Patro; mgr inż. Marcjjan Nowak Politechnika Częstochowska, Wydział Elektryczny, al. Armii Krajowej 17